AGU PUBLICATIONS

JGR

Journal of Geophysical Research: Earth Surface

RESEARCH ARTICLE
10.1002/2013JF003024

Key Points:
- Caddisfly silk nets are incorporated into a model of incipient sediment motion
- Silk nets increase critical shear stress in gravel-bedded streams
- Species-specific silk and behaviors control the range of grain sizes affected

Correspondence to:
L. K. Albertson,
lalbertson@stroudcenter.org

Citation:
Albertson, L. K., L. S. Sklar, P. Pontau, M. Dow, and B. J. Cardinale (2014), A mechanistic model linking insect (Hydropsychidae) silk nets to incipient sediment motion in gravel-bedded streams, *J. Geophys. Res. Earth Surf.*, *119*, 1833–1852, doi:10.1002/2013JF003024.

Received 28 OCT 2013
Accepted 19 AUG 2014
Accepted article online 23 AUG 2014
Published online 17 SEP 2014

A mechanistic model linking insect (Hydropsychidae) silk nets to incipient sediment motion in gravel-bedded streams

Lindsey K. Albertson[1], Leonard S. Sklar[2], Patricia Pontau[3], Michelle Dow[1], and Bradley J. Cardinale[3]

[1]Department of Ecology, Evolution, and Marine Biology, University of California, Santa Barbara, California, USA, [2]Department of Earth and Climate Sciences, San Francisco State University, San Francisco, California, [3]School of Natural Resources and Environment, University of Michigan, Ann Arbor, Michigan, USA

Abstract Plants and animals affect stream morphodynamics across a range of scales, yet including biological traits of organisms in geomorphic process models remains a fundamental challenge. For example, laboratory experiments have shown that silk nets built by caddisfly larvae (Trichoptera: Hydropsychidae) can increase the shear stress required to initiate bed motion by more than a factor of 2. The contributions of specific biological traits are not well understood, however. Here we develop a theoretical model for the effects of insect nets on the threshold of sediment motion, τ^*_{crit}, that accounts for the mechanical properties, geometry, and vertical distribution of insect silk, as well as interactions between insect species. To parameterize the model, we measure the tensile strength, diameter, and number of silk threads in nets built by two common species of caddisfly, *Arctopsyche californica* and *Ceratopsyche oslari*. We compare model predictions with new measurements of τ^*_{crit} in experiments where we varied grain size and caddisfly species composition. The model is consistent with experimental results for single species, which show that the increase in τ^*_{crit} above the abiotic control peaks at 40–70% for 10–22 mm sediments and declines with increasing grain size. For the polyculture experiments, however, the model underpredicts the measured increase in τ^*_{crit} when two caddisfly species are present in sediments of larger grain sizes. Overall, the model helps explain why the presence of caddisfly silk can substantially increase the forces needed to initiate sediment motion in gravel-bedded streams and also illustrates the challenge of parameterizing the behavior of multiple interacting species in a physical model.

1. Introduction

Recent work in geomorphology and ecology has shown that plants and animals can alter abiotic habitat characteristics such as atmospheric moisture [*Rixen and Mulder*, 2005; *Christner et al.*, 2008], flow regimes [*Hughes and Stachowicz*, 2004; *Katija and Dabiri*, 2009], and erosion rates [*Yoo et al.*, 2005; *De Baets et al.*, 2006]. In stream ecosystems, for example, riparian vegetation and activity by fish can influence channel morphology and sediment transport [*Flecker*, 1996; *Moore et al.*, 2004; *Braudrick et al.*, 2009]. However, despite the abundant evidence that organisms can affect morphodynamics of physical systems, there is still a lack of understanding of when and where these effects are most important and what biological attributes (e.g., population density, species traits, and species interactions) need to be considered in mechanistic models of geomorphic processes.

A key process in gravel-bedded streams is the onset of bed sediment motion with increasing shear stress. The shear stress required to initiate motion is important because it governs the frequency and intensity of bedload transport and thus influences many aspects of stream channel morphology [*Church*, 2006; *Parker et al.*, 2007]. Incipient motion is commonly quantified in terms of the critical value of the nondimensional Shields stress

$$\tau^* = \frac{\tau_b}{(\rho_s - \rho)gD} \quad (1)$$

where τ^*_{crit} is the Shields stress at incipient motion. In equation (1) τ_b is the average boundary shear stress, ρ_s and ρ_w are the densities of the sediment and water, respectively, g is the acceleration due to gravity, and D is the characteristic diameter of the bed surface sediments. For gravel and coarser sediments ($D > 2$ mm), τ^*_{crit} has been shown to be approximately constant with increasing grain size in hydraulically rough flow; values typically

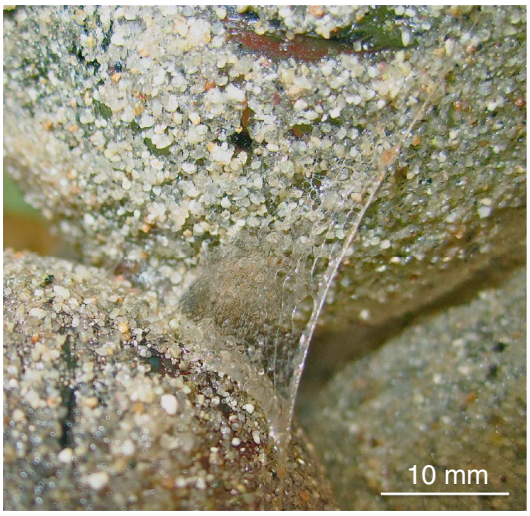

Figure 1. A caddisfly silk net built between two bed particles.

vary between 0.02 and 0.06 [*Buffington and Montgomery*, 1997]. Theoretical models have been developed to explain measured values of critical shear stress [*Wiberg and Smith*, 1987; *Bridge and Bennett*, 1992]; however, biological influences have not yet been incorporated. Abiotic explanations for the variability in τ^*_{crit} include sediment size distribution and packing geometry [*Kirchner et al*., 1990; *Komar and Carling*, 1991; *Wilcock*, 1993] and channel slope and relative roughness [*Mueller et al*., 2005; *Lamb et al*., 2008]. However, laboratory experiments suggest that benthic organisms can also play a significant role in controlling variation in critical shear stress [*Cardinale et al*., 2004; *Johnson et al*., 2009].

Benthic organisms such as caddisfly larvae in the net-spinning family Hydropsychidae (Trichoptera) can increase the shear stress required to initiate sediment motion by building silk webs between sediment grains [*Statzner et al*., 1999] (Figure 1). Although individual caddisfly larvae are small (<1 cm in length), the magnitude of their collective stabilizing effects could be large because they are one of the most abundant groups of aquatic insects in fast-flowing, riffle habitats. Hydropsychid benthic densities typically range from hundreds to thousands per square meter and have been shown to exceed 10,000 m^{-2} in some cases [*Miller*, 1984; *Cardinale et al*., 2004]. They are also an extremely widespread group, and multiple species are often found in the same stream. These species are aggressive toward one another and are known to compete for territory [*Englund and Olsson*, 1990; *Matczak and Mackay*, 1990]. In addition, there are large differences between species in net architecture and the locations where they choose to build their nets within stream substrates [*Loudon and Alstad*, 1992; *Harding*, 1997]. Each of these biological attributes may be important in understanding the magnitude and extent of caddisfly influence on initial sediment motion.

In a recent set of experiments, we found that hydropsychid caddisfly nets built on coarse gravel can increase τ^*_{crit} by more than a factor of 2 [*Albertson et al*., 2014]. The increase in τ^*_{crit} varied among different species when they were in monoculture, with a larger species, *Arctopsyche*, increasing τ^*_{crit} more than a smaller species, *Ceratopsyche*. We also found that the increase in sediment stability was amplified when the species were in polyculture assemblages. In the polyculture experiments, which were intended to better represent field conditions where multiple species coexist, we measured nonadditive increases in τ^*_{crit} above the expected average of the monoculture values, which we interpret to result from species interactions and partitioning of the benthic habitat [*Albertson et al*., 2014].

These results raise new questions about the potentially significant effects of benthic caddisfly larvae on sediment stability in stream channels. First, grain size has not been systematically varied in previous experiments [*Statzner et al*., 1999; *Cardinale et al*., 2004; *Johnson et al*., 2009; *Albertson et al*., 2014], which limits our ability to predict the range of grain sizes over which caddisfly nets may have an important effect on τ^*_{crit}. Second, to explain why different species produce differing effects on sediment stability, we need a better understanding of the influence of species-specific net characteristics, such as silk strength [*Loudon and Alstad*, 1992; *Brown et al*., 2004], thread spacing, net size, and the locations where insects build their nets. Finally, understanding how population density and species interactions affect sediment stability will be essential in translating laboratory results to complex field conditions.

To address these questions, we developed a theoretical model that incorporates caddisfly silk nets into mechanistic predictions of incipient sediment motion, using the *Wiberg and Smith* [1987] modeling framework applied to gravel-bedded rivers in temperate climates where caddisflies are typically abundant. The model accounts for the tensile forces that nets apply to bed surface grains at the threshold of motion, which depend on species-specific attributes such as net strength, vertical distribution of net locations, and the limits to population density due to size of organisms relative to grain size. To calibrate the model, we measured net tensile strength and other biological attributes for two common species of caddisfly, *Arctopsyche californica* and

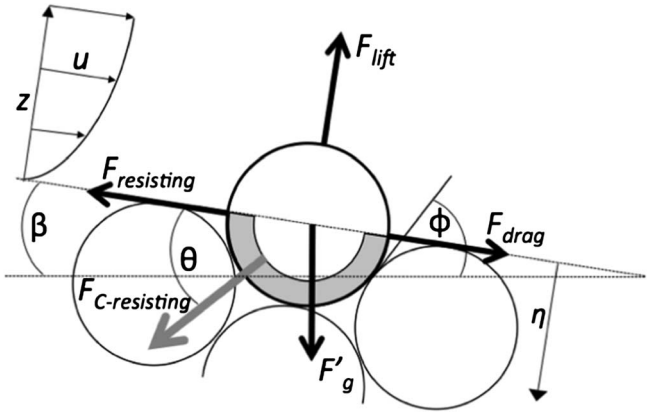

Figure 2. Definition sketch for model development. Incipient motion for a particle at the bed surface is controlled by four primary abiotic forces [*Wiberg and Smith*, 1987]. F_{drag}, F'_g, F_{lift}, and $F_{resisting}$ are the drag, buoyant gravitational, lift, and resisting forces, respectively; β is the slope of the bed, and ϕ is the friction angle. Fluid forces on the particle arise due to the velocity (u) profile with depth (z) above the grain. We added resisting forces generated by hydropsychid silk nets to this model by assuming that caddisflies build silk nets on the bottom half of the particle surface (gray shading) that contribute a binding force that resists downstream motion ($F_{C\_resisting}$). We define η as the depth below the bed surface where a caddisfly net is built and θ as the angle of the net with respect to the bed surface plane.

Ceratopsyche oslari. Finally, to test the model predictions, we build on our previous work [*Albertson et al.*, 2014] with new experiments that varied caddisfly species composition and grain size. Our goals are to determine (i) the range of grain sizes that are stabilized by caddisfly nets, (ii) the influence of variations in caddisfly density on τ^*_{crit}, (iii) the influence of species-specific differences in silk net characteristics, and (iv) the influence of species interactions in streams where multiple hydropsychid species coexist. Together, the model predictions and experimental results place bounds on the types of streams in which caddisfly nets are likely to influence sediment motion and provide new insight into the mechanistic links between animals and erosion in streams.

2. Model Development

In this section, we review the model developed by *Wiberg and Smith* [1987] that describes incipient sediment motion, or τ^*_{crit}, for a single grain at the bed surface of a stream. We then define the forces applied to sediment grains by caddisfly larvae silk nets and add the effects of caddisfly nets to the Wiberg and Smith model to derive an expression for τ^*_{crit} that explicitly accounts for the stabilizing effects of net density, net location, and silk thread strength. When defining the effects of nets, we first consider the forces applied to a sediment grain by an individual net and then consider the occurrence of multiple nets and the probability of their vertical locations by adding the areal density of insects and the depth profile of caddisflies into the model. After defining the forces exerted by nets on sediment grains, we evaluate the sensitivity of τ^*_{crit} to values of the biological parameters. In a later section, we consider how τ^*_{crit} varies with grain size when different caddisfly species are present alone or together.

2.1. Abiotic Framework

Wiberg and Smith [1987] derived a theoretical expression for τ^*_{crit} by balancing the sums of the driving and resisting forces acting on a grain in the direction parallel to the sloping sediment bed (Figure 2)

$$\Sigma F_{driving} = F_D + F'_g \sin\beta \tag{2}$$

$$\Sigma F_{resisting} = \left(F'_g \cos\beta - F_L\right) \tan\phi \tag{3}$$

where, F_D is the drag force due to flow across the grain, which acts in the downstream direction, and F_L is the lift force due to the vertical gradient in flow velocity, which acts normal to the bed. F'_g is the buoyant weight of the particle

$$F'_g = (\rho_s - \rho) g V_p = (\rho_s - \rho) g \pi D^3/6 \tag{4}$$

where V_p is the volume of the (nominally spherical) particle with diameter D, β is the slope angle of the bed with respect to the horizontal, and tan ϕ is a friction coefficient, where ϕ is the effective friction angle that depends on the geometry of the pocket that the grain rests within [*Kirchner et al.*, 1990]. F_D and F_L can be expressed as

$$F_D = \frac{C_D}{2} \tau_b \langle f^2\left(\frac{z}{z_0}\right)\rangle A_x \tag{5}$$

$$F_L = \frac{C_L}{2} \tau_b \left[f^2\left(\frac{z_T}{z_0}\right) - f^2\left(\frac{z_B}{z_0}\right)\right] A_x \tag{6}$$

Table 1. Parameter Values Used in Abiotic Reference Model (Equation (7))

Parameter	Value	Source
Channel slope β	0.5°	Assumed
Friction angle ϕ	60°	*Wiberg and Smith* [1987]
Drag coefficient C_D	0.76	*Schmeeckle et al.* [2007]
Ratio of lift to drag force	0.85	*Lamb et al.* [2008]
Shape factor α_D	1.5	*Wiberg and Smith* [1987]
von Karman's constant κ	0.407	*Wiberg and Smith* [1987]
$\langle f^2(z/z_0)\rangle$	38.3	Calculated[a]
Sediment density ρ_s	2500 kg/m^3	Assumed
Water density ρ	1000 kg/m^3	Assumed

[a]Calculated as $\left\{\left[\frac{1}{\kappa(D-z_0)}\right]\int_{z_0}^{D}\ln(z/z_0)dz\right\}^2$ assuming $\langle u(z)^2\rangle \approx \langle u(z)\rangle^2$ [*Smith and McLean*, 1984].

where C_D and C_L are the drag and lift coefficients, $f^2(z/z_0)$ is the square of the velocity profile function $f=\ln(z/z_0)/\kappa$, the pointed brackets indicate a vertically averaged quantity (in this case over the grain height), $\kappa=0.407$ is von Karman's constant, z is the local height above the mean bed elevation, subscripts T and B refer to the top and bottom of the grain, z_0 is a roughness parameter that represents the elevation where the velocity becomes zero, and A_x is the cross-sectional area of the grain over which the stress is applied; for hydraulically rough flow, $z_0=D/30$ [*Nikuradse*, 1933; *Wiberg and Smith*, 1987].

A particle is at the threshold of motion when the driving forces are equal to the resisting forces. The threshold of motion is determined by setting equation (2) equal to equation (3) and rearranging to obtain the expression for the nondimensional critical shear stress

$$\tau^*_{\mathrm{crit}} = \frac{2}{C_D\alpha_D}\frac{1}{\langle f^2(z/z_0)\rangle}\frac{(\tan\phi\cos\beta-\sin\beta)}{[1+(F_L/F_D)\tan\phi]} \tag{7}$$

where α_D is a dimensionless shape factor [*Wiberg and Smith*, 1987]. When we parameterize this expression with values appropriate for gravel-bedded rivers (Table 1), equation (7) gives $\tau^*_{\mathrm{crit}}=0.032$, which is at the low end of the range $0.03<\tau^*_{\mathrm{crit}}<0.06$ commonly measured in streams [*Buffington and Montgomery*, 1997]. This low value is appropriate for approximately planar beds lacking imbrication or complex sediment structures [*Buffington and Montgomery*, 1999]. Other equally appropriate parameterizations of equation (7) are possible, which might produce a higher value of τ^*_{crit}. Moreover, many of the simplifying assumptions implicit in equation (7) are not strictly correct, such as the assumption that the logarithmic velocity profile extends through the boundary layer at the bed [*Wiberg and Smith*, 1991; *Buffington and Montgomery*, 1999; *Schmeeckle et al.*, 2007; *Lamb et al.*, 2008]. Nevertheless, for our purposes, this parameterization provides a reasonable baseline value of τ^*_{crit} against which we can compare a version of the model that also includes the effects of caddisfly silk nets on incipient sediment motion.

2.2. Forces Applied by a Caddisfly Net

To incorporate the forces applied to bed particles by caddisfly nets into equation (7), we first consider the maximum force that a single net can sustain before breaking. A caddisfly net is composed of individual threads (Figure 3) that have a characteristic tensile strength (σ_T) and diameter (d) that vary with species. The individual threads will break at a tensile loading equal to the product of thread strength and cross-sectional area ($A_d=\pi d^2/4$). For simplicity, we assume that loading occurs in the net only in reaction to hydraulic forces applied to the grain and that strain on net threads is negligible prior to failure. We treat the total force-bearing capacity of an individual caddisfly net (F_{Ci}) as the sum of the force capacity of the individual threads carrying the load:

$$F_{\mathrm{Ci}} = N_T\sigma_T A_d = \frac{L_N\sigma_T\pi d^2}{4s} \tag{8}$$

where the number of load-bearing threads (N_T) is equal to the length of the mesh net structure (Figure 1) that is used for feeding (L_N) divided by the characteristic spacing between threads (s). Although there are reasons to expect that threads in a net might not all act additively, this assumption is a reasonable first approximation.

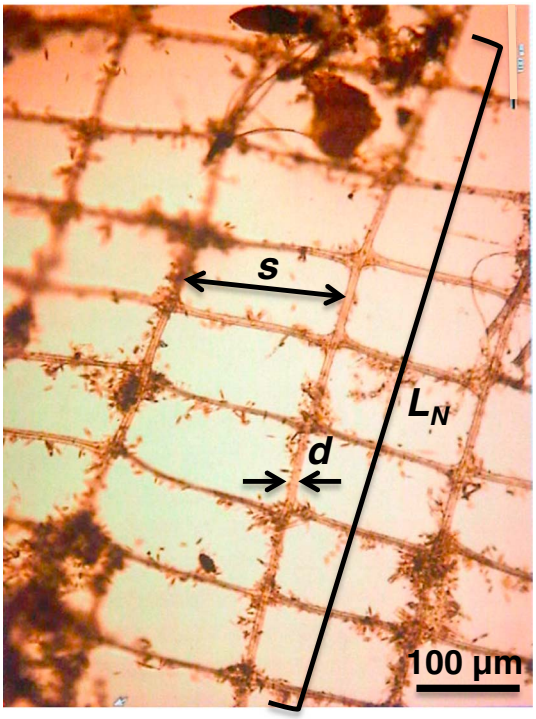

Figure 3. Caddisfly silk nets are composed of a series of threads that create a mesh structure that is used to filter food particles from the water column. Nets have a characteristic length (L_N), with a characteristic spacing (s) and diameter (d) of individual threads.

The contribution of a net to the force balance acting on a grain depends on where the net is attached to the grain and its orientation with respect to the grain surface and fluid forces. For simplicity we assume that the binding force of the net on the grain acts normal to the grain surface. Following *Wiberg and Smith* [1987], we consider only forces acting in the plane normal to the cross-stream direction and thus neglect lateral components of the forces acting on a grain. For this analysis we consider a grain protruding $D/2$ above neighboring grains of equal diameter, where $\phi = 60°$ and tan ϕ is 1.73. We define θ as the angle of the net with respect to the bed surface plane, such that nets can be attached anywhere along the semicircle from $\theta = 0$ to 180° because the focal grain is protruding (Figure 2).

F_{Ci} contributes to the forces resisting grain motion in two ways. The component of F_{Ci} parallel to the bed surface ($F_{Ci} \cos \theta$), and oriented in the upstream direction ($0 \le \theta \ge 90$), contributes to the resisting forces by directly opposing fluid drag. We assume that the downstream component parallel to the bed does not add to the driving forces because forces arise in the nets only in reaction to fluid loading. The component of F_{Ci} normal to the bed ($F_{Ci} \sin \theta$) opposes the hydraulic lift force and thus contributes to the frictional resistance to motion. Hence we can write

$$F_{Ci\_resisting} = F_{Ci}(\cos\theta + \sin\theta \tan\phi) \quad (0 \le \theta \le 90) \tag{9}$$

$$F_{Ci\_resisting} = F_{Ci} \sin\theta \tan\phi \quad (90 \le \theta \le 180) \tag{10}$$

The magnitudes of the bed-parallel and bed-normal components of F_{Ci} vary nonlinearly with depth below the bed surface (η, 0 at surface, positive below, negative above surface; Figure 2), because

$$\theta = \sin^{-1}\left(\frac{2\eta}{D}\right) \tag{11}$$

We can use equation (11) and trigonometric identities to restate equations (9) and (10) in terms of η

$$F_{Ci\_resisting} = F_{Ci}\left(\sqrt{1-(2\eta/D)^2} + (2\eta/D)\tan\phi\right) (\text{for } 0 \le \theta \le 90) \tag{12}$$

$$F_{Ci\_resisting} = F_{Ci}(2\eta/D)\tan\phi \quad (\text{for } 90 \le \theta \le 180) \tag{13}$$

Nets built on the upstream side of a grain ($0 \le \theta \le 90$) should resist sediment motion more effectively than nets built on the downstream side of that grain ($90 \le \theta \le 180$). We assume for simplicity that caddisflies are equally likely to build nets on the upstream versus downstream sides of the grain. We can account for the odds of a net occurring on the upstream or downstream sides of a grain by combining equations (12) and (13) and giving half-weight to the bed-parallel term:

$$F_{Ci\_resisting} = F_{Ci}\left(\frac{\sqrt{1-(2\eta/D)^2}}{2} + (2\eta/D)\tan\phi\right) \quad (\text{for } 0 \le \eta \le D/2) \tag{14}$$

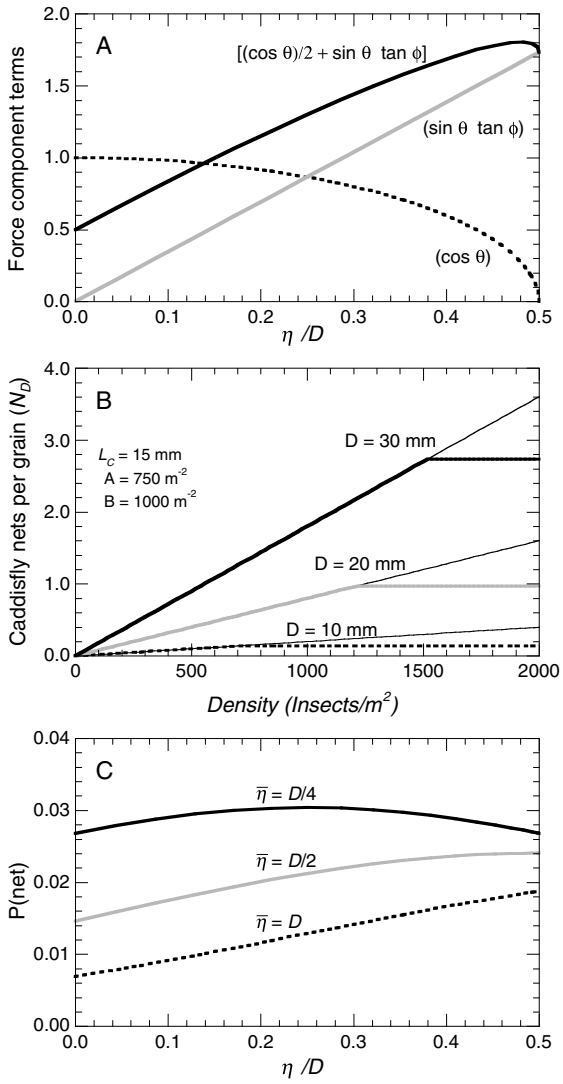

Figure 4. Variation in model components. (a) Variation in trigonometric terms that control the resisting force of caddisfly nets as a function of dimensionless depth below the bed surface (η/D), with depth normalized by grain diameter over the range of depths from the bed surface ($\eta = 0$) to the bottom of the focal grain ($\eta = D/2$): (cos θ) = tensile bed-parallel component; (sin θ tan ϕ) = frictional bed-normal component (equation (10)); and (1/2 cos θ + sin θ tan ϕ) = combined frictional and tensile components, where the factor 1/2 accounts for the fact that only nets attached to the upstream side of grain provide tensile resistance to particle motion (equation (14)). (b) Variation in number of caddisfly nets per grain N_D as a function of areal density (equation (15)) taking into account the pore size limitation (equation (17)) for three grain sizes; here insect length $L_C = 15$ mm, $A = 750\ \mathrm{m}^{-2}$, and $B = 1000\ \mathrm{m}^{-2}$. For each grain size there are two curves: the continuously sloping lines represent the potential areal density given the pore size limitation, and the constant value lines represent an arbitrary areal density of insects where grain size and thus pore size are sufficiently large so that other factors are limiting. (c) Distributions of potential net depths (equation (19)) for three mean depths.

The bed-normal term receives full weight because this force component occurs whether the net is upstream or downstream of the focal grain. This probabilistic approach underestimates the potential stabilizing force when nets are on the upstream side and overestimates for nets on the downstream side but should be representative of the resisting force averaged across multiple grains in a setting where multiple nets are evenly distributed between upstream and downstream sides.

The variation in the trigonometric terms that control the bed-parallel, bed-normal, and combined force components are shown in Figure 4a, where the depth below the bed surface η is normalized by grain diameter D. Although nets may be built at depths below $D/2$, they would not be attached to the protruding grain; hence, net forces resisting motion drop to zero at the depth $\eta > D/2$.

2.3. Areal Density of Caddisfly Nets

In section 2.2, we defined an expression for the average resisting forces applied by a single caddisfly net, but it is likely that multiple nets could be acting on a single grain at the bed surface. The number of nets attached to a given grain will depend on the density of insects and the size of the grain relative to the size of the insect so that the pore spaces created by grains are suitable for net construction. Insect density is typically quantified as the number of individuals per unit bed area (I_A) and is often estimated in the field by kicknet or Surber samples taken from a known area [*Hauer and Lamberti*, 2007]. Hydropsychid density is controlled by a variety of factors, including dispersal ability [*Sharpe and Downes*, 2006], food availability [*Englund*, 1993], and flow conditions [*Hildrew and Edington*, 1979]. In this model, we do not make assumptions about all of the factors controlling hydropsychid density but simply calculate how many nets are acting on an average grain across a range of caddisfly densities.

To express the areal density of nets as the number of nets per sediment grain (N_D), we make the following assumptions: each insect builds one net, each net is attached to two grains, and the effective bed surface area occupied by a grain (A_D) scales with the square of grain diameter ($A_D = \pi D^2/4 \approx D^2$). Thus, we can write

$$N_D = 2 I_A A_D = 2 I_A D^2 \qquad (15)$$

Equation (15) shows that for a given areal hydropsychid density I_A, larger grains are likely to have a greater number of nets attached. On the other hand, there should be a limit to the areal density of insects that a bed can accommodate as grain sizes become smaller. This limit likely arises because of the scaling between insect body size and the size of pore spaces between grains. When grains are small and pore space size is limiting, hydropsychid densities are typically lower, which potentially occurs because individuals drift to find more suitable locations [*Mihuc et al*., 1996; *Kerans et al*., 2000].

To model the pore size limitation on hydropsychid occupancy, we define a maximum potential areal caddisfly density I_{AP} and consider it a function of the ratio of grain diameter D to insect body length L_C. We expect that the dependence of I_{AP} on D/L_C will be nonlinear and continuous, approaching limits of occupancy where grain diameter and body length are of similar magnitude (D/L_C ~1). When $D/L_C >> 1$, other factors such as food supply or current velocity are likely to limit areal density, so that only a fraction of the potential capacity of the substrate is utilized (i.e., $I_A < I_{AP}$). In the absence of any relationships between sediment sizes and hydropsychid densities in the literature, we parameterize the pore limitation on caddisfly density as a linear-logarithmic function of D/L_C

$$I_{AP} = A\ln\left(D/L_C\right) + B \tag{16}$$

where the slope parameter A controls the sensitivity of I_{AP} to D/L_C and the intercept parameter B is the potential areal density when $D = L_C$. Equation (16) predicts that potential caddisfly density drops to zero when $D/L_c = \exp(-B/A)$. This logarithmic formulation is consistent with the assumption that potential density is most sensitive to D/L_C when insect lengths are similar to grain diameter, with steadily declining effects of pore size as D/L_C grows large. Combining equations (15) and (16) for the case where areal density is limited by pore size (i.e., $I_A = I_{AP}$), we calculate N_D as

$$N_D = 2D^2[A\ln(D/L_C) + B] \tag{17}$$

Figure 4b shows how N_D varies with I_A for various grain diameters, when, for illustration, $L_C = 15$ mm, $A = 750$ insects m^{-2}, and $B = 1000$ insects m^{-2}.

Caddisflies may also choose not to build nets on small sediment particles when grain diameters are small relative to the size of the net that a given species typically builds. Based on qualitative field observations that caddisflies build smaller nets on smaller sediments but that net size becomes approximately constant for larger sediments, we assume that net attachment length becomes limited when the grain diameter is less than 3 times the typical attachment length L_N. The grain-limited attachment length L_{ND} is thus

$$L_{ND} = D/3 \quad (\text{for } D \le 3L_N) \tag{18}$$

2.4. Vertical Distribution of Caddisfly Nets

In addition to the hydropsychid areal density, we considered the vertical distribution of nets with depth within the substrata. Caddisflies typically occupy pore spaces and build nets within and on the surface layer as well as at depths below $D/2$ [*Harding*, 1997]. We assume that only nets attached to surface grains will contribute to resisting particle motion. Based on observations of the vertical distributions in previous work [*Albertson et al*., 2014], we assume that the probability of encountering a net at a given depth follows a normal distribution, where $\overline{\eta}$ and S_η are the mean and standard deviation of the distribution of the net depths:

$$P(\text{net}) = \frac{N_D e^{-(\eta-\overline{\eta})^2/2S_\eta^2}}{S_\eta\sqrt{2\pi}\left[1 - \frac{1}{S_\eta\sqrt{2\pi}}\int_{-\infty}^{0} e^{-(\eta-\overline{\eta})^2/2S_\eta^2}\mathrm{d}\eta\right]} \tag{19}$$

where the distribution is truncated at the surface ($\eta = 0$) and normalized so that the integral of equation (19) is equal to N_D. Figure 4c shows hypothetical vertical distributions of hydropsychid net locations for three grain sizes, for the case where $\overline{\eta}$ varies around D while S_η is held constant at $D/2$ mm [*Albertson et al*., 2014].

2.5. Effect of Multiple Nets on Threshold Particle Motion

To account for areal density and depth variation in quantifying the contribution of caddisfly nets to the forces acting on individual sediment grains, we adopt a probabilistic approach. We assume that forces affecting the average surface grain can be represented by the integral over the grain depth ($0 \le \eta \le D/2$) of the product of

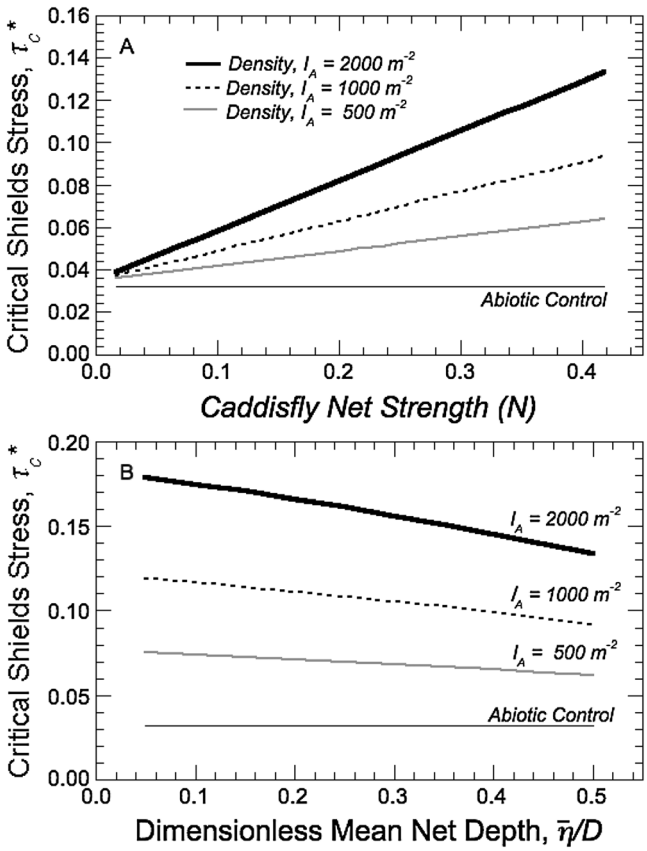

Figure 5. Model predictions for critical Shields stress, τ^*_{crit}, as a function of caddisfly net strength and the ratio of net depth to rock size over a range of caddisfly densities. (a) Critical Shields stress increases linearly as caddisfly net strength increases for low (500 m^{-2}), intermediate (1000 m^{-2}), and high (2000 m^{-2}) caddisfly densities. Grain diameter and the mean and standard deviation of the net depths are held constant at 20 mm, 20 mm, and 10 mm, respectively. (b) Critical Shields stress declines as the mean net depth moves from the grain's midpoint to its bottom. Silk strength is held constant at 0.2 N.

the P(net) distribution from equation (19), the probability of a net occurring at a given depth, and $F_{Ci}(\eta)$, the force that a single net at that depth would apply to a grain

$$F_{c\_resisting} = \int_0^{D/2} P(\text{net}) F_{Ci}(\eta) \mathrm{d}\eta \tag{20}$$

Following the algebraic manipulations of *Wiberg and Smith* [1987], we can now express nondimensional critical shear stress as the sum of the physical and caddisfly net forces:

$$\tau^*_{\text{crit}} = \frac{2}{C_D \alpha_D} \frac{1}{\langle f^2(z/z_0) \rangle} \frac{\left(\tan\ \phi \cos\ \beta - \sin\ \beta + F_{C\_\text{resisting}}/F_g^{'}\right)}{[1 + (F_L/F_D)\tan\ \phi]} \tag{21}$$

The model predicts that τ^*_{crit} will be sensitive to caddisfly density. As shown in Figures 5a and 5b, for realistic densities of 500–2000 hydropsychids m^{-2}, the model predicts τ^*_{crit} values within the range of 0.032–0.16 that has been measured in natural streams [*Buffington and Montgomery*, 1997]. As caddisfly net strength increases, τ^*_{crit} increases linearly (Figure 5a). τ^*_{crit} is also sensitive to the vertical distribution of caddisfly nets attached to a grain, decreasing gradually as the mean of the vertical net distribution shifts toward the bottom of the surface grain (Figure 5b). Thus, the integrated contribution of possible net locations to $F_{C\_\text{resisting}}$ is substantial along the entire depth of the grain but maximized when nets are concentrated toward the bed surface.

In summary, we have modified a standard model of incipient sediment motion to include the biological forces applied by silk nets spun by caddisfly larvae to surface grains in gravel-bedded rivers. The biological

Table 2. Biotic Model Parameters

Parameter	Source	*Arctopsyche californica*	*Ceratopsyche osalri*
Silk thread tensile strength σT	this study	15 ± 1.5 MPa	7.2 ± 0.7 MPa
Silk thread diameter d	this study	0.0250 ± 0.0006 mm	0.0177 ± 0.0007 mm
Number of load-bearing threads per silk net N_T	this study	16.3 ± 0.9	36.6 ± 1.5
Length of silk net L_N	this study	7.6 ± 0.5 mm	7.3 ± 0.3 mm
Spacing between silk threads s	this study	18.98 ± 0.93	11.72 ± 0.53
Forced sustained by a silk net F_{Ci}	this study	0.120 ± 0.013 N	0.066 ± 0.004 N
Mean silk net depth below bed surface	*Albertson et al.* [2014]	22.0 ± 1.1 mm	29.0 ± 1.3 mm
Insect body length L_C	*Albertson et al.* [2014]	17.6 ± 0.2 mm	7.8 ± 0.1 mm
Potential caddisfly density sensitivity A	this study	750 m^{-2}	750 m^{-2}
Potential caddisfly density intercept B	this study	1000 m^{-2}	1000 m^{-2}

parameters that are included in the revised model are silk thread strength, thread diameter, thread spacing, net length, areal density of caddisflies, and the mean and standard deviation of the vertical distribution of nets within benthic substrata. Each of these parameters is likely to vary by species. Because the model includes only one abiotic variable, grain diameter, we can calibrate the biological parameters but allow grain diameter to vary, which allows us to make predictions about the threshold of motion when caddisflies are present in streams with a given grain size distribution. In the next section of the manuscript, we use laboratory and field measurements to calibrate each of the biological parameters for two common caddisfly species. We then use experiments to test how the model performs in predicting the effect of caddisfly nets on τ^*_{crit} across grain sizes.

3. Silk Net Characteristics

To apply the model that we developed in section 2 to a natural system in which different species of caddisfly are present in the same stream, we measured a suite of caddisfly silk net characteristics for two common species of caddisfly.

3.1. Study System

Caddisflies are abundant in gravel-bedded streams in the Sierra Nevada where much of our research has been performed. Two species, *Arctopsyche californica* and *Ceratopsyche oslari*, are particularly abundant in streams near the University of California's Sierra Nevada Aquatic Research Laboratory in Mammoth Lakes, CA, where past experiments have been conducted [*Leland et al*., 1986]. To calibrate the model for *Arctopsyche* and *Ceratopsyche* silk nets, we estimated silk thread length, diameter, and strength for two study species that vary in body size and net-building locations [*Albertson et al*., 2014].

3.2. Silk Thread Characteristics

Intact silk nets built by *Arctopsyche* and *Ceratopsyche* were collected from McGee (latitude 37°35′N, longitude 118°47′W) and Convict Creeks (latitude 37°36′N, longitude 118°49′W) near Mammoth Lakes, CA, by carefully removing them from rocks by hand and gently placing each net in a 50 mL falcon tube. Nets were stored in filtered (0.2 μm) stream water at 1°C in a portable freezer and transported to the laboratory at the University of California, Santa Barbara. Within 24 h, silk nets were isolated from most debris using a dissecting microscope (Leica M80 Stereomicroscope) and scalpel. During this process, for each of the fully intact nets isolated, the number of silk threads, the diameter of three representative silk threads, and the length and width of the net were measured using Leica Application Suite software (Version 3.7.0). A total of 25 *Arctopysche* and 30 *Ceratopsyche* nets were measured (Table 2).

3.3. Silk Tensile Strength Calibration

After the silk mesh was isolated, we performed a stress analysis to measure the tensile strength of the nets. Stress analysis was performed on an MTS Systems Corporation Bionix 200 universal testing machine at a nominal strain rate of 4 mm min^{-1}, using a 50 N load cell and a built-in optical encoder to measure the load (in newtons) when the net broke. All nets were tested at room temperature in deionized water using a custom-made stainless-steel cup (10 cm deep; 6 cm diameter). Each net was pulled to breaking. The system

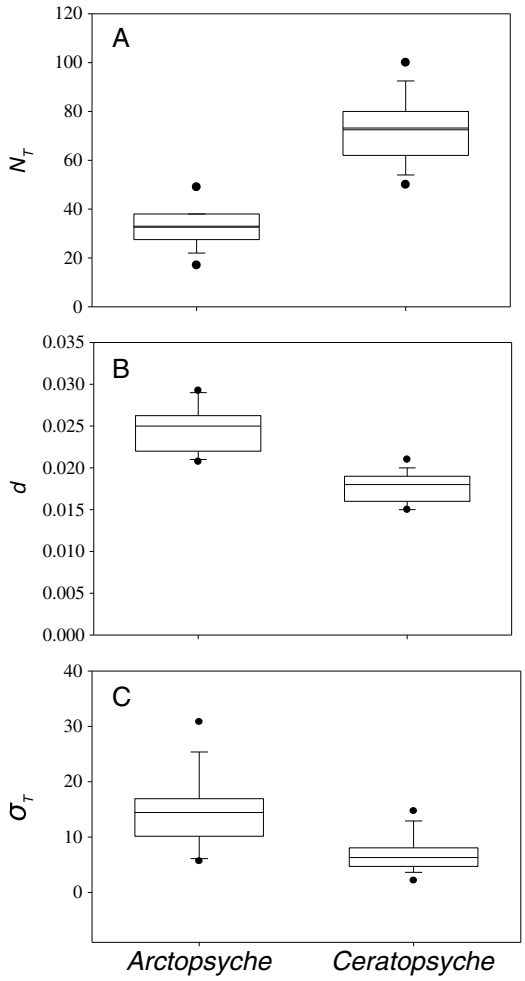

Figure 6. Measurements of caddisfly net characteristics for two species common in the Sierra Nevada, CA, USA. *Arctopsyche* nets have (a) fewer but (b) thicker and (c) stronger silk threads than *Ceratopsyche*. Boxes represent the 25th and 75th percentiles, whiskers represent the 5th and 95th percentiles, and outliers are solid circles.

was then reset in between each of $N = 28$ and $N = 30$ replicate nets for *Arctopysche* and *Ceratopsyche*, respectively.

As hypothesized, there were significant differences in net characteristics between the two caddisfly species (Table 2 and Figures 6a–6c). *Arctopsyche* nets had significantly fewer threads than *Ceratopsyche* nets (*t* test: $p < 0.001$), averaging 16.3 ± 0.9 and 36.6 ± 1.5 for the two species, respectively (Figure 6a). *Arctopsyche* nets also had thicker threads than *Ceratopsyche* nets ($p < 0.001$; Figure 6b), but there was no significant difference in total net area ($p = 0.16$) for the two species, even though *Arctopsyche* nets were 15% larger, averaging 50 mm^2 for *Arctopsyche* and 42 mm^2 for *Ceratopsyche*. *Arctopsyche* net threads were also significantly stronger than *Ceratopsyche* threads ($p < 0.001$), averaging 15 ± 1.5 and 7.2 ± 0.7 MPa for the two species, respectively (Figure 6c). When we measured the maximum tensile force that could be sustained by a full net for each species (equation (8)), we found that *Arctopsyche* silk nets were 25% stronger than *Ceratopsyche* silk nets ($p = 0.048$), averaging 0.12 N and 0.066 N, respectively. We used values from these measurements of silk net strengths to parameterize and test the model of incipient grain motion from section 2.

4. Measuring Incipient Motion With Caddisflies Present

After we calibrated the model that was developed in section 2 using silk tensile strength measurements that were reported in section 3, we conducted a laboratory experiment that simultaneously manipulated the presence and absence of two caddisfly species and grain size to test the effects of caddisfly nets on the incipient motion of sediments of different size. Our goal was to experimentally test the model predictions to determine the range of grain sizes over which caddisfly silk nets likely increase τ^*_{crit} in streams. In this section, we report results in two steps. First we use the experiment to characterize caddisfly areal density and vertical distribution and the remaining biological factors for the theoretical model and use the fully parameterized model to predict the effects of various treatments on τ^*_{crit}. We then use experimental measurements of incipient motion and the associated shear stresses when caddisflies are present or absent to compare model predictions to the observed values of τ^*_{crit}.

4.1. Experimental Design

We experimentally manipulated caddisfly species composition and grain size in laboratory flumes to compare our model predictions to experimental results. We used a set of four clear plexiglass flumes (1.2 m long × 0.15 m wide × 0.20 m deep) housed at the Sierra Nevada Aquatic Research Laboratory (SNARL) for the experiment, which ran from 12 April and 4 June 2013. Water was recirculated in each flume by a direct current motor (Bodine) attached to a stainless-steel shaft with a 10 cm diameter propeller in the return circulation pipe below the downstream end of the flume [*Albertson et al.*, 2014,

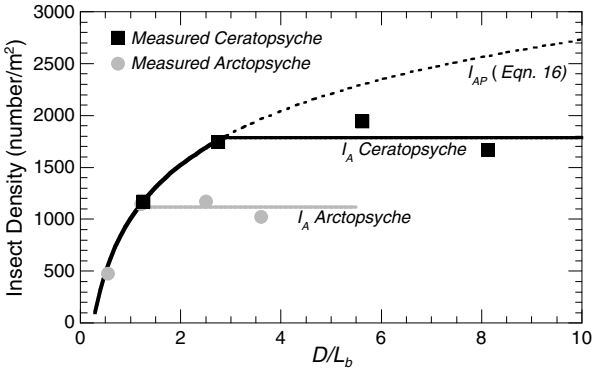

Figure 7. Density of *Ceratopsyche* and *Arctopsyche* in monoculture in the laboratory experiment. Density was lowest in the 10 mm treatment for both species. In the three larger grain size treatments, density for *Ceratopsyche* averaged 1700 m^{-2} and for *Arctopsyche* averaged 1000 m^{-2}. These data were used to parameterize the values of *A* and *B* in the pore limitation function in the model (equation (16)). Dashed line shows potential areal density; solid lines show predicted densities where not limited by pore size.

Figure 1b]. After passing through the propeller, flow traveled more than 1 m through the return pipe and was passed through a turbulence diffusor at the entrance of the flume, before traveling another 0.9 m to the test section. This length is equivalent to about 20 times the flow depth, sufficient distance for any large-scale turbulent structure set up by the propeller to be diffused. Additionally, the 0.90 m approach to the test section was sufficient to develop a stable boundary layer in the lower portion of the flow, resulting in consistent log linear velocity profiles in the near-bed region (section 4.5). The flow was controlled by adjusting propeller speed using a speed control console (Minarik). Water in the flumes came from nearby Convict Creek and was maintained at ambient stream temperatures (17–19°C).

The experiment was designed as a randomized block in which each of four caddisfly treatments was randomly assigned to each of four flumes during temporal blocks. The four caddisfly treatments were as follows: (i) a control with no caddisflies, (ii) a monoculture of *Arctopsyche*, (iii) a monoculture of *Ceratopsyche*, and (iv) a 50:50 polyculture of *Arctopsyche* and *Ceratopsyche*. Each flume was then randomly assigned to one of four bed surface conditions in which grain size varied. The four grain size treatments were composed of uniform sediments with a surface *D* of natural, rounded grains equal to 10, 22, 45, or 65 mm. To simulate a bed with a coarse surface layer [*Lisle*, 1995] as commonly observed at our field sites, we installed the surface grain layer over a uniform subsurface grain layer with a *D* equal to one half the surface *D*. A coarse surface layer produces a natural gradient of larger pore spaces closer to the bed surface and smaller pore spaces at depth. This is relevant to the different caddisfly species, which vary in body size, and hence the pore spaces through which they can move and build silk nets. Each grain size × caddisfly composition treatment was replicated 5 times over the course of the experiment. At the start of each temporal block, the sediments were installed in a 0.15 m × 0.10 m recessed test section in each flume. The sediment patch was located 90 cm downstream from the flume entrance to allow full flow acceleration. Grains were placed by hand into the sediment patches resulting in a relatively loose packing arrangement. The grains were subsequently water-worked during the caddisfly colonization period described below, producing minor shifts in particle position and weak imbrication. The loose, uniform grain sizes used in our experiments are not representative of typical field conditions in which wide grain size distributions allow development of complex sediment structures or interlocked grains [*Church et al.*, 1998a, 1998b]. Nevertheless, our experimental surfaces could be considered similar to natural gravel beds with narrow size distributions of recently deposited (loose) sediments or textural patches having such characteristics.

4.2. Caddisfly Colonization

At the beginning of each temporal block, the sediment patches were populated by placing caddisfly larvae into the water column just upstream of the test section and allowing them to settle into the sediments. The target hydropsychid density was 2000 m^{-2}, which is in the range of densities commonly found in nearby streams and other gravel-bedded rivers [*Leland et al.*, 1986; *Cardinale et al.*, 2004; *Albertson et al.*, 2011]. After drifting into the sediment patch, larvae were given a 4 day colonization period, which allowed enough time for them to both search for a suitable location to settle and build a complete silk net (see example in Figure 1). During this time, the larvae were fed pulverized algae wafers (Hikari) at a concentration of $>$ 50 particles/mL once per day [*Cardinale and Palmer*, 2002; *Cardinale et al.*, 2002]. When individuals drifted past the sediment patch, they were recirculated through the flume until settling occurred.

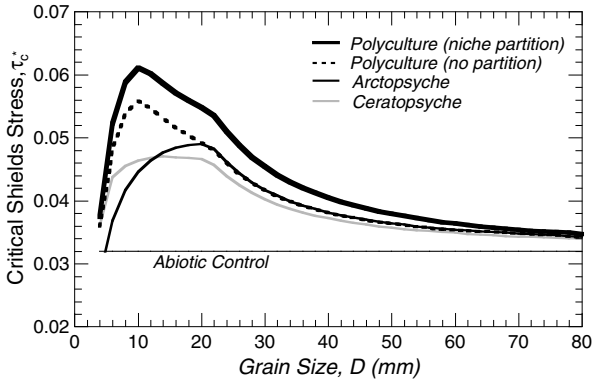

Figure 8. The model predicted that caddisflies would increase the threshold of sediment motion and that this stabilizing effect would decrease exponentially as grain size increased. We parameterized the model (see section 2.1 for prediction of control value = 0.032) with silk strengths measured for two common caddisfly species, *Arctopsyche californica* and *Ceratopsyche oslari* (see Figure 6). Model simulations for situations when both species were present, but did not vertically partition space, showed a nonadditive increase in caddisfly effects on incipient sediment motion only for grains smaller than 20 mm. Model simulations for situations when both species were present and did vertically partition space showed a nonadditive increase in the threshold of sediment motion across all grain sizes.

4.3. Caddisfly Density Across Grain Sizes

Although caddisflies were introduced to the sediment patches at a density of 2000 m^{-2}, some individuals never settled or died, so final settling density varied across grain sizes and species. Because final caddisfly settling density could not be estimated during the colonization period without disturbing the caddisfly silk nets, final density was measured during the simulated flood described below by catching and enumerating any drifting caddisflies in a net downstream of the test section. We found that caddisfly density was substantially lower for both species in the smallest (10 mm) grain size treatment (Figure 7), which we represent in the model by calibrating the pore space limitation function in equation (17) with these data; equation (16) encloses the data well with $A = 750\ m^{-2}$ and $B = 1000\ m^{-2}$. In the three larger grain size treatments (where $I_A < I_{AP}$), caddisfly densities averaged 1700 m^{-2} for *Ceratopsyche* and 1100 m^{-2} for *Arctopsyche*. In the polyculture treatments, the caddisflies consistently settled at a 3:2 ratio of *Ceratopsyche* to *Arctopsyche* across all grain sizes, with mean values of 900 m^{-2} and 600 m^{-2}, respectively, for a combined density of 1500 m^{-2}.

4.4. Model Predictions Using Measured Densities and Vertical Distributions

We completed the parameterization of the theoretical model using the measured mean caddisfly densities and observations from a complementary study specifically designed to document vertical net locations [*Albertson et al.*, 2014]. Based on those observations, the peak of the vertical net distribution was placed at the grain bottom, $\overline{\eta} = 0.5D$, and the spread of the distribution was $S_\eta = 0.5D$ in the model simulations for the caddisfly monoculture treatments.

Model predictions for critical Shields stress under these experimental conditions are shown in Figure 8. Comparing the two monoculture treatments, the model predicts that both species should increase τ^*_{crit} by nearly 50%, with *Arctopsyche* nets increasing the threshold of sediment motion more than *Ceratopsyche* for grain sizes larger than approximately 12 mm (Figure 8). This is likely due to the stronger silk present in *Arctopsyche* nets (Figure 6c). The effects of both species on sediment mobility decline exponentially with increasing grain size, decreasing to within 7% of the abiotic control for grains larger than 70 mm.

We ran model simulations for two polyculture scenarios. In the first scenario, we assumed that both species are present and their net distributions stay the same as in monoculture with a mean net depth $\overline{\eta} = 0.5D$ and $S_\eta = 0.5D$. In the second, we assumed that both species are present but they compete for and partition space, which is an interaction that has been documented in previous studies [*Matczak and Mackay*, 1990; *Harding*, 1997; *Albertson et al.*, 2014]. For this simulation, we made the simplifying assumption that the larger species and superior competitor *Arctopsyche* occupied a shallower range of depths within the substrate ($\overline{\eta} = 0.375D$ and $S_\eta = 0.25D$) and that the smaller species *Ceratopsyche* was displaced to a deeper range of depths where $\overline{\eta} = 0.625D$. For both species, niche partitioning results in a narrow range of depths occupied ($S_\eta = 0.25D$) as we have documented in a complementary study [*Albertson et al.*, 2014]. With this parameterization of the vertical separation of the two hydropsychid species due to niche partitioning, the model predicts a substantial increase in the critical shear stress, with a maximum roughly double the abiotic control at $D = 10$ mm. Niche partitioning also increases τ^*_{crit} compared to the case when no interactions between species were assumed. This effect is maximized for grains with D between 10 and 25 mm, declining exponentially as grain size increased above 25 mm (Figure 8).

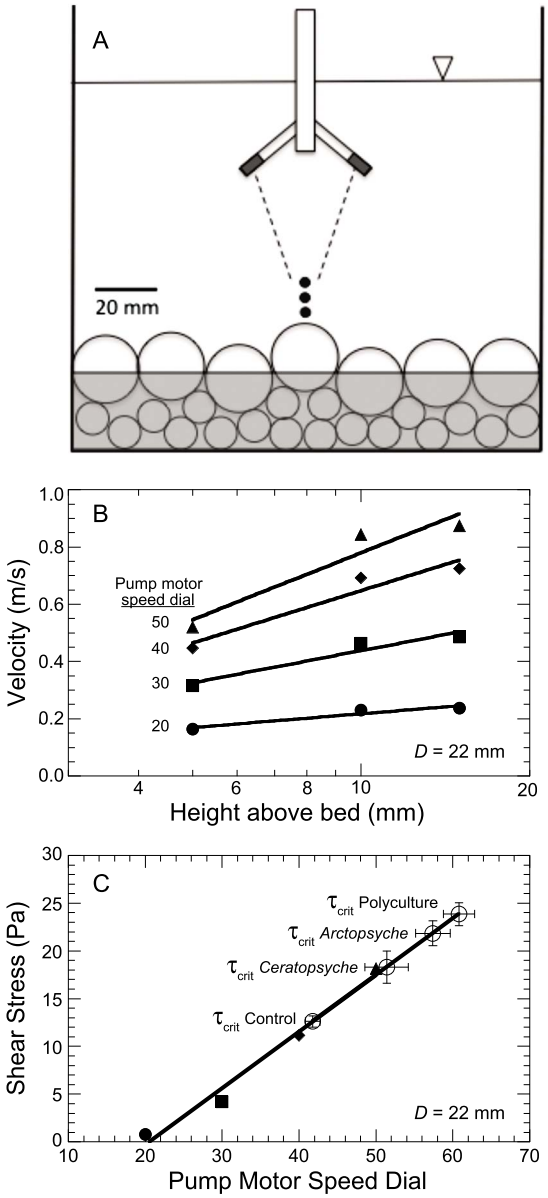

Figure 9. Estimating shear stress from vertical velocity profiles. (a) Flume cross-section schematic for $D = 22$ mm, showing Nortek Vectrino ADV, and sampling points 5, 10, and 15 mm above bed, and flow depth of 110 mm. Gray shaded region containing 10 mm subsurface grains is portion of test section below plexiglass floor of flume. Grain packing arrangement shown for illustration only. (b) Velocity profiles for $D = 22$ mm, for various pump motor speed dial settings; grains glued to bed to prevent motion at high shear stresses. (c) Calibration curve for $D = 22$ mm, showing shear stress calculated from velocity profiles (solid symbols as in Figure 9b) and estimated critical shear stress for four treatments based on the dial setting where initial motion occurred (open circles; error bars are standard errors from replicate experiments).

4.5. Estimating Shields Stress

After the colonization period, we simulated the rising limb of a flood event to test whether the threshold shear stress for sediment motion was different in sediment patches containing (i) caddisfly monocultures versus the controls with no caddisflies, (ii) the average of the caddisfly monocultures versus the polyculture with both species, and (iii) how both of these outcomes varied across a range of grain sizes over which caddisfly nets potentially influence critical shear stress. To do this, we gradually increased flow velocity by incrementing motor dial speed until we visually observed at least one rock moving out of the test patch into a 1 mm mesh net located 5 cm downstream. The visual criterion of first movement has been widely used in previous laboratory studies of initial sediment motion [*Buffington and Montgomery*, 1997].

To estimate the bed shear stress at initial sediment motion, we constructed a calibration curve relating the dial speed setting on the pump motor to the bed shear stress calculated from measurements of vertical velocity profiles for each grain size. Velocity profiles were measured over sediment patches of each grain size with a surface layer identical to that in the experiment, but the grains were cemented together so that we could obtain stable measurements of velocity and shear stresses at and above the critical value without grains moving. As shown in Figure 9a, we measured velocity profiles above the center of each patch using an Acoustic Doppler Velocimeter (Nortek Vectrino) at increasing motor dial speeds and calculated shear stress as

$$\tau_b = \rho_w \left(\kappa \frac{\partial u}{\partial (\ln z)} \right)^2 \tag{22}$$

where $\frac{\partial u}{\partial (\ln z)}$ is the slope of the logarithmic vertical velocity profile [*Wilcock*, 1996; *Gordon et al.*, 2004]. Velocity profiles were log linear within the lower 20% of the flow depth (Figure 9b). We did not use velocity measurements at higher elevations above the bed, or away from the flume center line, to avoid wall effects which produce lateral velocity gradients. We then used linear regressions between pump motor speed dial settings and boundary shear stress for each grain size to estimate the critical shear stress from the dial settings where initial motion occurred. Figure 9c shows results for $D = 22$ mm. We quantify initial motion from movement of the first particle(s) displaced, which were generally entrained from the center of the channel where the shear stresses were greatest. Therefore, while our estimates of shear stress are not applicable across the entire channel, they do provide an

Table 3. Results of the Mixed Effects Model That Was Used to Analyze the Experiment

Model	Fixed Effect[a]	d.f.[b]	F[c]	p[d]
Full	Grain size	1, 67	410	< 0.001
	Caddisfly treatment	3, 67	9.2	< 0.001
	Caddisfly density	1, 67	8.63	< 0.001
	Grain size × caddisfly treatment	3, 67	0.88	0.46
Reduced	Grain size	1, 70	412	< 0.001
	Caddisfly treatment	3, 70	9.21	< 0.001
	Caddisfly density	1, 70	8.67	0.004
Model comparisons		AIC[e]	L Ratio[f]	p[d]
Full		532.1		
Reduced		528.0	2.92	0.4

[a]Variable manipulated.
[b]Degrees of freedom.
[c]F statistic.
[d]Probability statistic.
[e]Akaike information criteria.
[f]Likelihood ratio.

appropriate empirical estimate of the stresses driving the observed initial motion. Critical shear stress values were then converted to Shields stress.

4.6. Data Analysis for the Experiment

Measurements of critical Shields stress in the experiment were compared across treatments using general linear mixed models in which the threshold of sediment motion was a function of the fixed effects of grain size, caddisfly treatment, and caddisfly density and the random effect of replicate. Analyses that included the interaction between grain size and caddisfly treatment as a covariate (Table 3) suggest that conclusions did not depend on the interaction term (grain size × treatment: $p = 0.46$). Thus, it was not included in further statistical modeling. Grain size, caddisfly treatment, and caddisfly density were all significant predictor variables of critical shear stress (Table 3). Within each of the four grain sizes used in the experiment, we used pairwise contrasts corrected for multiple comparisons to test for differences in Shields stress between (i) the control with no caddisflies and caddisfly monocultures and (ii) the average of the monocultures and the polyculture treatment for measured values of τ^*_{crit}. Due to low replication of each caddisfly treatment × grain size combination ($N = 5$), we accepted differences with $p \leq 0.1$ as significant. Models were fit using the lme4 package in R 2.9.0.

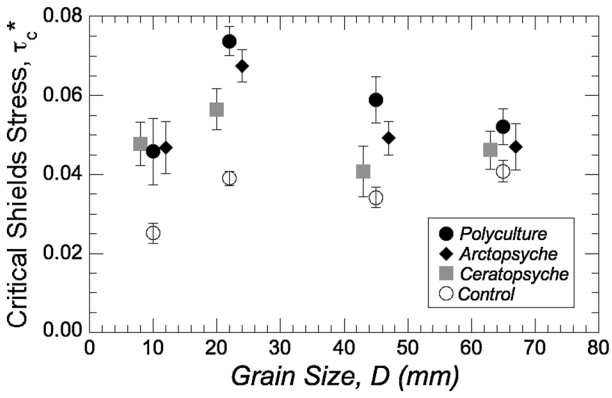

Figure 10. Results of an experiment that measured shear stress at the threshold of sediment motion when two caddisfly species were present alone or together (polyculture) compared to controls without caddisflies across a range of grain sizes. Caddisflies significantly increased the threshold of motion for 10, 22, and 45 mm grains but not 65 mm grains. Nonadditive increases of both species together in τ^*_{crit} were observed for grain sizes between 22 and 45 mm. Values are means ± 1 SE and are jiggered about the four grain size values for graphing purposes.

4.7. Experimental Results

Given the expectation that τ^*_{crit} is independent of grain size for hydraulically rough flow [*Buffington and Montgomery*, 1997], we predicted a constant value of τ^*_{crit} for the abiotic control treatments across grain size. Although there is an apparent trend in our measurements of τ^*_{crit} with grain size for the control treatments without caddisflies present (Figure 10 and Table 4), the relationship is not significant (linear regression: $R^2 = 0.42$, $p = 0.35$). Furthermore, the τ^*_{crit} values for the control treatments are in the range of 0.03 to 0.04, as expected

Table 4. Results of the Experiment That Measured τ^*_{crit}, the Nondimensional Critical Shear Stress

	τ^*_{crit}[a]			
Treatment	10 mm	22 mm	45 mm	65 mm
Control[b]	0.028 ± 0.002	0.040 ± 0.002	0.034 ± 0.003	0.041 ± 0.003
Ceratopsyche[c]	0.044 ± 0.004	0.056 ± 0.005	0.041 ± 0.006	0.046 ± 0.005
Arctopsyche[d]	0.044 ± 0.005	0.067 ± 0.004	0.049 ± 0.004	0.047 ± 0.006
Polyculture[e]	0.043 ± 0.006	0.072 ± 0.004	0.059 ± 0.006	0.052 ± 0.005

[a]Values are means for $N = 5$ replicates ± 1 SE.
[b]Sediments with no caddisflies.
[c]Sediments with *Ceratopsyche oslari* present.
[d]Sediments with *Arctopsyche californica* present.
[e]Sediments with both species present.

for loosely packed grains in hydraulically rough flow [*Buffington and Montgomery*, 1997]. When we pooled the τ^*_{crit} response values for all treatments in which caddisflies were present in the sediments, we found an increase in the threshold of sediment motion compared to the control sediments that did not have caddisflies. These increases were significant with 90% confidence for grain diameters of 10 mm ($p = 0.013$), 22 mm ($p < 0.001$), and 45 mm ($p = 0.07$) but not for 65 mm ($p = 0.19$) rocks (Figure 10). Values of τ^*_{crit} for the polyculture treatments were significantly higher than the additive expectation (the average of the monocultures) for the 22 mm ($p = 0.004$) and 45 mm ($p = 0.018$) treatments but not for 10 mm ($p = 0.96$) or 65 mm ($p = 0.65$). Thus, nonadditive effects of polycultures were only detected over an intermediate range of grain sizes (approximately 22–45 mm). These results suggest that the mobility of grains larger than 65 mm is unlikely to be affected by caddisfly silk nets and that the effects of hydropsychid species interactions in polycultures are maximized for streams where the grain size is in the range between 22 and 45 mm.

4.8. Comparing the Model and the Experiment

To compare the model with the experimental results, we calibrated the abiotic component of the model so that model predictions match experimental observations for the abiotic control values of τ^*_{crit} for each grain size. This allows us to focus on the biologically driven influence of caddisfly nets on critical Shields stress without the confounding effects of variability in the abiotic reference value of τ^*_{crit}. Although we found no systematic variation in abiotic τ^*_{crit} with grain size, we suspect that the differences could be due in part to variations in the grain packing with grain size, which may have occurred due to the narrow width of the flume. Such variability could be accounted for in the model by varying effective friction angle ϕ. Using the friction angle as a tuning parameter, we obtain an exact match between model and experimental abiotic τ^*_{crit} values with $\phi = 53°$, 73°, 64°, and 75° for $D = 10$ mm, 22 mm, 45 mm, and 65 mm, respectively, a deviation of no more than 25% from the uniform value of 60° used above.

Comparison of model predictions and experimental observations are shown in Figure 11. The model accurately predicted the quantitative effects of caddisfly silk nets on sediment mobility in the laboratory experiment. Both model and experiment showed the greatest absolute values of τ^*_{crit} for sediment grains of 22 mm diameter (Figures 10 and 11a). Although we only examined four sediment sizes, the observed and predicted values of τ^*_{crit} were similar and highly correlated for *Ceratopsyche* in monoculture ($r = 0.99$) and *Arctopsyche* in monoculture ($r = 0.95$) (Figures 11a and 11b). Model predictions of τ^*_{crit} differed most from observed for the polyculture treatment, particularly for $D = 45$ mm ($r = 0.37$) (Figure 11c). We hypothesize that the discrepancy in predicted versus observed results may be due to factors not accounted for in the model, including variable silk strength and size across caddisfly species treatments, the potential influence of silk retreats which contain additional silk material, or adhesion properties of silk at the end of threads that directly contact the grain surface.

To assess the overall significance of the presence of the caddisflies nets on sediment stability, we calculated the ratio of treatment τ^*_{crit} to abiotic control, which varied with grain size. We found that the caddisfly monocultures showed the strongest increases in τ^*_{crit} for 10 and 22 mm grains (Figures 11d and 11e), with a steady decline as grain size increased. In monoculture, nets increased critical Shields stress by up to a factor of 1.6 for *Ceratopsyche* on 10 mm grains and 1.7 for *Arctopsyche* on 22 mm grains. The strongest effects of caddisfly nets relative to the abiotic control were in the polyculture treatment (Figure 11f), with τ^*_{crit} increasing by a factor of 1.8 for grains between 22 and 45 mm in diameter, with less substantial increases for the 10 and 65 mm grains.

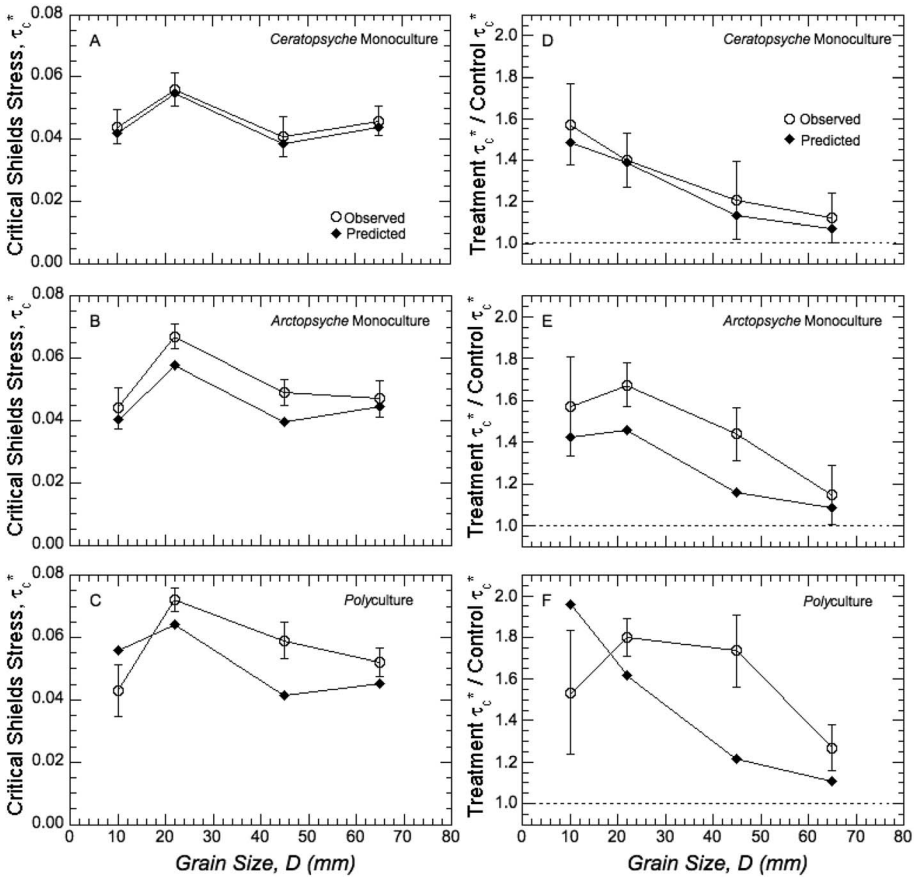

Figure 11. Comparisons of observed experimental values of τ^*_{crit} with predictions of the model that is parameterized with experimentally measured insect densities and silk net strengths. Absolute values of τ^*_{crit} for assessing model accuracy for caddisfly (a, b) monocultures and (c) polycultures. τ^*_{crit} values relative to abiotic controls to assess the significance of the caddisfly nets in (d, e) monoculture and (f) polyculture. Error bars are ± 1 SE.

5. Discussion

An increasing number of studies have investigated how organisms can influence the magnitude and heterogeneity of current speeds and sediment movement in streams [*Schulz et al.*, 2003; *Johnson et al.*, 2011; *Rice et al.*, 2012; *Statzner*, 2012]. However, there is still a lack of information that defines the range of conditions where organisms have the greatest effect on physical processes. Here we have incorporated the tensile binding forces of caddisfly silk nets into a widely used model of incipient sediment motion to determine the range of grain sizes over which caddisfly nets are predicted to increase the force needed to initiate grain motion. Based on results from previous studies, we predicted that the effects of caddisflies on incipient motion would be maximal for gravels with a *D* in the range of 10–45 mm and that these effects would be sensitive to caddisfly density, species identity, and species interactions [*Johnson et al.*, 2009; *Albertson et al.*, 2014]. Our model results are consistent with each of these predictions and provide a mechanistic basis for predicting the range of conditions where benthic animal structures in streams could measurably influence sediment transport. This work supports previous findings that animals and plants can substantially affect a variety of sediment transport processes, including sediment erosion and deposition [*Yoo et al.*, 2005; *Braudrick et al.*, 2009].

To parameterize the model, we measured the tensile strength of silk from nets built by two common species of caddisfly and found that *Arctopsyche* silk nets were 25% stronger, on average, than *Ceratopsyche* nets. The net strength measurements for these two species (7.5–15 MN/m^2) were substantially lower than those previously reported for other hydropsychid caddisfly species (221 MN/m^2) [*Brown et al.*, 2004], which may be due to differences in the strength of silk produced by different species or differences in the net strength measurement methodology. We assumed that nets were spatially distributed according to previous findings in the laboratory [*Albertson et al.*, 2014], but net locations as well as the relationships between the density or

size of nets with respect to grain size still need to be measured in the field. Although the model provides insights into the forces acting on grains at the bed surface, it does not include the potential for the clustering of grains, which could occur if hydropsychid nets bind several particles together at depth so that they respond as one collective grain. Clustering is likely to occur when nets are built below the bed surface and could potentially influence τ^*_{crit} if the effective size of a grain is increased.

The results of the experimental manipulation generally supported the model predictions, and both support previous findings that caddisfly nets increase the forces needed to initiate rock motion [*Statzner et al*., 1999; *Cardinale et al*., 2004; *Johnson et al*., 2009]. In our experiment, caddisfly nets were able to increase the threshold of sediment motion for grains smaller than 65 mm. In monoculture, caddisfly effects relative to abiotic controls were maximized for 10 and 22 mm diameter grains but sustained for grains up to 45 mm in diameter. The diminished effect of caddisflies on incipient motion for 10 mm grains compared to 22 mm grains for the *Arctopsyche* monoculture and polyculture treatments likely resulted from (i) a reduction in caddisfly density resulting from downstream drift that is initiated when body size exceeds pore space size and suitable habitat to build nets is lacking and (ii) a change in the size of nets when attachment sites on the surfaces of small grains for the silk nets are reduced. The diminishing effect at 65 mm for all caddisfly treatments likely resulted from the inherent scale effect that limits the influence of nets on particles much larger than insect size. Net resistance is small relative to the abiotic forces required to move large grains and, for constant insect density, becomes insignificant for large particles.

In support of previous findings, we found experimental evidence that treatments with two caddisfly species increased the threshold of motion more than the additive effects of each species alone for the 22 and 45 mm grain sizes [*Albertson et al*., 2014]. Caddisflies are a diverse group of organisms, and it is common for several species to coexist as mixtures [*Loudon and Alstad*, 1992]. Different species are also known to partition space, such that some species build nets in locations close to the bed surface, while others build nets deeper within the sediments [*Albertson et al*., 2014; *Harding*, 1997]. The model predicts smaller effects on τ^*_{crit} for 22 to 65 m grain sizes in polyculture than were actually observed, which may be because the model does not include grain clustering when hydropsychid nets bind together many grains below the bed surface due to vertical habitat partitioning. These results suggest that interactions between species can be important for incipient sediment motion but may be limited to streams dominated by grain sizes within the range of 22–45 mm for which our model would predict a significant effect of caddisfly polycultures on the threshold of sediment motion. Further work is warranted to investigate the influence of more than two coexisting species on incipient sediment motion. Given the small number of case studies that have explicitly monitored the effects of diversity on abiotic processes [*Hughes and Stachowicz*, 2004; *Rixen and Mulder*, 2005; *Allen and Vaughn*, 2011], more studies are needed to draw conclusions about the generality of these diversity effects.

Although the flumes used in our experiment provided a simple representation of natural stream conditions, they allowed us to directly test our model predictions and isolate the effects of benthic organisms on sediment motion, which would be difficult to accomplish in the field. Because all of our calculations and comparisons were made relative to controls that had no caddisflies, we are certain that the results reveal relative, if not absolute, effects of caddisflies on sediment movement. Field experiments are the logical next step for testing model predictions under more natural conditions. Monitoring changes in τ^*_{crit} in streams where caddisfly density and diversity vary due to differences in predator abundance or food quality would provide an interesting extension of the current work [*Statzner*, 2012]. Because caddisflies both influence and are affected by sediment motion, feedbacks between physical and biological processes may be important in this system [*Moore*, 2006; *Albertson et al*., 2011]. Very few studies have considered how species traits or species interactions in ecological communities affect physical processes where temporal and spatial variation in physical-biological feedbacks are influenced by the composition of communities [*Widdows et al*., 2000; *Murray et al*., 2008; *Viles et al*., 2008; *Fuller et al*., 2012].

6. Conclusion

Both biological and physical processes can regulate important ecosystem functions like erosion regimes, habitat formation, nutrient cycling, and productivity, but the relative strengths of these processes are debated [*Dietrich and Perron*, 2006]. Here we have explicitly incorporated two common animal species into a standard model of initial sediment motion and find that caddisfly larvae may have larger effects on the erosion of a broader range

of gravel sizes (~10–45 mm) than previously anticipated. This effect is sensitive to variation in the density and species composition of the animal assemblage, and our findings highlight the importance of understanding species-specific traits like silk net tensile strength. These findings also confirm the need for field experiments that incorporate realistic species assemblages to mechanistically link biological organisms to incipient sediment motion. Recent synthesis papers have emphasized the need to mechanistically link life and its landscape [*Palmer and Bernhardt*, 2006; *Reinhardt et al*., 2010], and our results further suggest that models that do not incorporate biological effects might substantially underestimate the forces required to move streambed material.

Notation

A_d	cross-sectional area of threads (mm^2)
A_D	area occupied by individual grain (mm^2)
α_D	shape factor
B	potential areal caddisfly density (insects/m^2)
C_D	drag coefficient
C_L	lift coefficient
D	grain diameter (mm)
d_i	diameter of threads (mm)
F_{Ci}	force bearing capacity of net (N)
F_D	drag force (N)
F_g'	buoyant weight of grain (N)
F_L	lift force (N)
I_A	gravitational acceleration (m/s^2)
I_{AP}	caddisfly areal density (individuals/m^2)
κ	von Karman's constant
L_C	caddisfly body length (mm)
L_N	length of net (mm)
β	bed slope (deg)
$\overline{\eta}$	mean net depth (mm)
η	net depth (mm)
N_D	pore limited caddisfly density (individuals/m^2)
N_T	number of threads in tension
ρ	density of water (kg/m^3)
ρ_s	density of sediment (kg/m^3)
P(net)	distribution of nets
ϕ	particle friction angle (deg)
s	spacing between threads (mm)
S_η	deviation of net distribution (mm)
σ_T	tensile strength of silk (MPa)
τ^*_{crit}	nondimensional critical shear stress
τ_b	boundary shear stress (Pa)
θ	angle of repose
u	velocity (m/s)
z	local height above the bed (mm)
z_B	height of grain bottom (mm)
z_0	elevation where velocity becomes zero (mm)
z_T	height of grain top (mm)

Acknowledgments
We thank D. Albertson and M. Mohamed for field assistance and H. Waite, Y. Tan, and J. Calendar for help with the tensile strength measurements. S. Cooper and T. Dunne generously provided insightful comments on previous drafts of this manuscript. Data from this paper are available from the authors. Funding was provided to L.K.A by the Valentine Eastern Sierra Reserve, the National Center for Earth Surface Dynamics, and the National Science Foundation (1110571). Participation by L.S.S. was supported by the SFSU Dawdy Fund for Hydrologic Sciences.

References

Albertson, L. K., B. J. Cardinale, S. C. Zeug, L. R. Harrison, H. S. Lenihan, and M. A. Wydzga (2011), Impacts of channel reconstruction on invertebrate assemblages in a restored river, *Restor. Ecol.*, *19*(5), 627–638.

Albertson, L., B. J. Cardinale, and L. S. Sklar (2014), Species interactions generate non-additive increases in sediment stability in laboratory streams, *PLoS One*, *9*(8), e103417, doi:10.1371/journal.pone.0103417.

Allen, D. C., and C. C. Vaughn (2011), Density-dependent biodiversity effects on physical habitat modification by freshwater bivalves, *Ecology*, *92*(5), 1013–1019.
Braudrick, C. A., W. E. Dietrich, G. T. Leverich, and L. S. Sklar (2009), Experimental evidence for the conditions necessary to sustain meandering in coarse-bedded rivers, *Proc. Natl. Acad. Sci. Am.*, *106*(40), 16,936–16,941.
Bridge, J. S., and S. J. Bennett (1992), A model for the entrainment and transport of sediment grains of mixed sizes, shapes, and densities, *Water Resour. Res.*, *28*(2), 337–363, doi:10.1029/91WR02570.
Brown, S. A., G. D. Ruxton, and S. Humphries (2004), Physical properties of *Hydropsyche siltalai* (Trichoptera) net silk, *J. North Am. Benthol. Soc.*, *23*(4), 771–779.
Buffington, J. M., and D. R. Montgomery (1997), A systematic analysis of eight decades of incipient motion studies, with special reference to gravel-bedded rivers, *Water Resour. Res.*, *33*(8), 1993–2029, doi:10.1029/96WR03190.
Buffington, J. M., and D. R. Montgomery (1999), Effects of hydraulic roughness on surface textures of gravel-bed rivers, *Water Resour. Res.*, *35*, 3507–3521, doi:10.1029/1999WR900138.
Cardinale, B. J., and M. A. Palmer (2002), Disturbance moderates biodiversity-ecosystem function relationships: Experimental evidence from caddisflies in stream mesocosms, *Ecology*, *83*(7), 1915–1927.
Cardinale, B. J., M. A. Palmer, and S. L. Collins (2002), Species diversity enhances ecosystem functioning through interspecific facilitation, *Nature*, *415*(6870), 426–429.
Cardinale, B. J., E. R. Gelmann, and M. A. Palmer (2004), Net spinning caddisflies as stream ecosystem engineers: The influence of *Hydropsyche* on benthic substrate stability, *Funct. Ecol.*, *18*, 381–387.
Christner, B. C., C. E. Morris, C. M. Foreman, R. Cai, and D. C. Sands (2008), Ubiquity of biological ice nucleators in snowfall, *Science*, *319*(5867), 1214.
Church, M. (2006), Bed material transport and the morphology of alluvial river channels, *Annu. Rev. Earth Planet. Sci.*, *34*, 325–354.
Church, M., M. A. Hassan, and J. F. Wolcott (1998a), Stabilizing self-organized structures in gravel-bed stream channels: Field and experimental observations, *Water Resour. Res.*, *34*(11), 3169–3179, doi:10.1029/98WR00484.
Church, M., M. A. Hassan, and J. F. Wolcott (1998b), Stabilizing self-organized structures in gravel-bed stream channels: Field and experimental observations, *Water Resour. Res.*, *34*(11), 3169–3179, doi:10.1029/98WR00484.
De Baets, S., J. Poesen, G. Gyssels, and A. Knapen (2006), Effects of grass roots on the erodibility of topsoils during concentrated flow, *Geomorphology*, *76*(1–2), 54–67.
Dietrich, W. E., and J. T. Perron (2006), The search for a topographic signature of life, *Nature*, *439*(7075), 411–418.
Englund, G. (1993), Effects of density and food availability on habitat selection in a net spinning caddis larva, *Hydropsyche siltalai*, *Oikos*, *68*, 473–480.
Englund, G., and T. Olsson (1990), Fighting and assessment in the net-spinning caddis larvae *Arctopsyche ladogensis*: A test of the sequential assessment game, *Anim. Behav.*, *39*, 55–62.
Flecker, A. (1996), Ecosystem engineering by a dominant detritivore in a diverse tropical ecosystem, *Ecology*, *77*, 1845–1854.
Fuller, B. M., L. S. Sklar, Z. G. Compson, K. J. Adams, J. C. Marks, and A. C. Wilcox (2012), Ecogeomorphic feedbacks in regrowth of travertine step-pool morphology after dam decommissioning, Fossil Creek, Arizona, *Geomorphology*, *126*(314–322), 732–740.
Gordon, N. D., T. A. McMahon, B. L. Finlayson, C. J. Gipple, and R. J. Nathan (2004), *Stream Hydrology: An Introduction for Ecologists*, John Wiley, England, U. K.
Harding, J. S. (1997), Strategies for coexistence in two species of New Zealand Hydropsychidae (Trichoptera), *Hydrobiologia*, *350*, 25–33.
Hauer, F. R., and G. A. Lamberti (2007), *Methods in Stream Ecology*, Elsevier, Burlington, Mass.
Hildrew, A. G., and J. M. Edington (1979), Factors facilitating the coexistence of hydropsychid caddis larvae (Trichoptera) in the same river system, *J. Anim. Ecol.*, *48*(2), 557–576.
Hughes, A. R., and J. J. Stachowicz (2004), Genetic diversity enhances the resistance of a seagrass ecosystem to disturbance, *Proc. Natl. Acad. Sci. U.S.A.*, *101*(24), 8998–9002.
Johnson, M. F., I. Reid, S. P. Rice, and P. J. Wood (2009), Stabilization of fine gravels by net-spinning caddisfly larvae, *Earth Surf. Process. Landforms*, *34*(3), 413–423.
Johnson, M., S. Rice, and I. Reid (2011), Increase in coarse sediment transport associated with disturbance of gravel river beds by signal crayfish (*Pacifastacus leniusculus*), *Earth Surf. Process. Landforms*, *36*, 1680–1692.
Katija, K., and J. O. Dabiri (2009), A viscosity-enhanced mechanism for biogenic ocean mixing, *Nature*, *460*(7255), 624–626.
Kerans, B. L., P. L. Chesson, and R. A. Stein (2000), Assessing density-dependent establishment and dispersal: An example using caddisfly larvae, *Can. J. Fish. Aquat. Sci.*, *57*(6), 1190–1199.
Kirchner, J., W. E. Dietrich, F. Iseya, and H. Ikeda (1990), The variability of critical shear stress, friction angle, and grain protrusion in water-worked sediments, *Sedimentology*, *37*, 647–672.
Komar, P. D., and P. A. Carling (1991), Grain sorting in gravel-bed streams and the choice of particle sizes for flow-competence evaluations, *Sedimentology*, *38*(3), 489–502.
Lamb, M. P., W. E. Dietrich, and J. G. Venditti (2008), Is the critical Shields stress for incipient sediment motion dependent on channel-bed slope?, *J. Geophys. Res.*, *113*, F02008, doi:10.1029/2007JF000831.
Leland, H. V., S. V. Fend, J. L. Carter, and A. D. Mahood (1986), Composition and abundance of periphyton and aquatic insects in a Sierra Nevada, California, stream, *Great Basin Nat.*, *46*, 595–611.
Lisle, T. (1995), Particle size variations between bed load and bed material in natural gravel bed channels, *Water Resour. Res.*, *31*(4), 1107–1118, doi:10.1029/94WR02526.
Loudon, C., and D. N. Alstad (1992), Architectural plasticity in net construction by individual caddisfly larvae (Trichoptera: Hydropsychidae), *Can. J. Zool.*, *70*(6), 1166–1172.
Matczak, T. Z., and R. J. Mackay (1990), Territoriality in filter-feeding caddisfly Larvae: Laboratory experiments, *J. North Am. Benthol. Soc.*, *9*(1), 26–34.
Mihuc, T. B., G. W. Minshall, and J. R. Mihuc (1996), Species-environment relationships among filter-feeding caddisflies (Trichoptera: Hydropsychidae) in Rocky Mountain streams, *Great Basin Nat.*, *56*(4), 287–293.
Miller, J. (1984), Competition, predation, and catchnet differentiation among net-spinning caddisflies (Trichoptera), *Oikos*, *43*, 117–121.
Moore, J. W. (2006), Animal ecosystem engineers in streams, *BioScience*, *56*(3), 237–246.
Moore, J. W., D. E. Schindler, and M. D. Scheuerell (2004), Disturbance of freshwater habitats by anadromous salmon in Alaska, *Oecologia*, *139*(2), 298–308.
Mueller, E. R., J. Pitlick, and J. M. Nelson (2005), Variation in the reference Shields stress for bed load transport in gravel-bed streams and rivers, *Water Resour. Res.*, *41*, W04006, doi:10.1029/2004WR003692.

Murray, A. B., M. A. F. Knaapen, M. Tal, and M. L. Kirwan (2008), Biomorphodynamics: Physical-biological feedbacks that shape landscapes, *Water Resour. Res.*, *44*, W11301, doi:10.1029/2007WR006410.
Nikuradse, J. (1933), Laws of flow in rough pipes, *VDI-Forschungsheft*, *361*, 1–63.
Palmer, M. A., and E. S. Bernhardt (2006), Hydroecology and river restoration: Ripe for research and synthesis, *Water Resour. Res.*, *42*(3), W03S07, doi:10.1029/2005WR004354.
Parker, G., P. R. Wilcock, C. Paola, W. E. Dietrich, and J. Pitlick (2007), Physical basis for quasi-universal relations describing bankfull hydraulic geometry of single-thread gravel bed rivers, *J. Geophys. Res.*, *112*, F04005, doi:10.1029/2006JF000549.
Reinhardt, L., D. Jerolmack, B. J. Cardinale, V. Vanacker, and J. Wright (2010), Dynamic interactions of life and its landscape: Feedbacks at the interface of geomorphology and ecology, *Earth Surf. Process. Landforms*, *35*(1), 78–101.
Rice, S. P., M. F. Johnson, and I. Reid (2012), Animals and the geomorphology of gravel-bed rivers, in *Gravel-Bed Rivers: Processes, Tools, Environments*, edited by M. Church, P. M. Biron, and A. G. Roy, pp. 225–241, John Wiley, Chichester, U. K.
Rixen, C., and C. P. H. Mulder (2005), Improved water retention links high species richness with increased productivity in arctic tundra moss communities, *Oecologia*, *146*(2), 287–299.
Schmeeckle, M. W., J. M. Nelson, and R. L. Shreve (2007), Forces on stationary particles in near-bed turbulent flows, *J. Geophys. Res.*, *112*, F02003, doi:10.1029/2006JF000536.
Schulz, M., H.-P. Kozerski, T. Pluntke, and K. Rinke (2003), The influence of macrophytes on sedimentation and nutrient retention in the lower River Spree (Germany), *Water Res.*, *37*(3), 569–78.
Sharpe, A., and B. J. Downes (2006), The effects of potential larval supply, settlement and post-settlement processes on the distribution of two species of filter-feeding caddisflies, *Freshw. Biol.*, *51*, 717–729.
Smith, J., and S. McLean (1984), A model for flow in meandering streams, *Water Resour. Res.*, *20*(9), 1301–1315, doi:10.1029/WR020i009p01301.
Statzner, B. (2012), Geomorphological implications of engineering bed sediments by lotic animals, *Geomorphology*, *157*, 49–65.
Statzner, B., M. F. Arens, J. Y. Champagne, R. Morel, and E. Herouin (1999), Silk-producing stream insects and gravel erosion: Significant biological effects on critical shear stress, *Water Resour. Res.*, *35*(11), 3495–3506, doi:10.1029/1999WR900196.
Viles, H. A., L. A. Naylor, N. E. A. Carter, and D. Chaput (2008), Biogeomorphological disturbance regimes: Progress in linking ecological and geormorphological systems, *Earth Surf. Process. Landforms*, *33*(9), 1419–1435.
Wiberg, P., and J. Smith (1991), Velocity distribution and bed roughness in high-gradient streams, *Water Resour. Res.*, *27*(5), 825–838, doi:10.1029/90WR02770.
Wiberg, P. L., and J. D. Smith (1987), Calculations of the critical shear stress for motion of uniform and heterogeous sediments, *Water Resour. Res.*, *23*(8), 1471–1480, doi:10.1029/WR023i008p01471.
Widdows, J., M. D. Brinsley, P. N. Salkeld, and C. H. Lucas (2000), Influence of biota on spatial and temporal variation in sediment erodability and material flux on a tidal flat (Westerschelde, The Netherlands), *Mar. Ecol. Ser.*, *194*, 23–37.
Wilcock, P. R. (1993), Critical shear stress of natural sediments, *J. Hydraul. Eng.*, *119*(4), 491–505.
Wilcock, P. R. (1996), Estimating local bed shear stress from velocity observations, *Water Resour. Res.*, *32*(11), 3361–3366, doi:10.1029/96WR02277.
Yoo, K., R. Amundson, A. M. Heimsath, and W. E. Dietrich (2005), Process-based model linking pocket gopher (Thomomys bottae) activity to sediment transport and soil thickness, *Geology*, *33*(11), 917–920.